*34th EPS Conference on Plasma Phys. Warsaw, 2 - 6 July 2007 ECA Vol.**31F**, P-4.163 (2007)*

An assessment of ITER scenarios under varying assumptions of NBI capability and NBCD code benchmark

T. Oikawa[1], A.R. Polevoi[1], V. Mukhovatov[1], M. Shimada[1],
D.J. Campbell[1], V. Chuyanov[1], K. Tani[2]
[1]*ITER Organization, St Paul lez Durance, France*
[2]*JAEA, Naka, Japan*

1. NBI capability under various design possibilities

The ITER NBI is defined in the FDR 2001 to have 2 injectors with a beam energy (E_B) of 1 MeV and an injection power (P_{inj}) of 16.5 MW. Reduction of the beam energy is currently under discussion for increasing the plasma rotation in terms of suppressing MHD instabilities. The NBI capability therefore has been assessed for various design possibilities.

The first wall heat load is limited to 0.5MW/m^2. The NB power density on the far wall has the maximum of 50 MW/m^2 on the beam axis without attenuation in a plasma. Thus tolerable shinethrough is up to 1 %. The electron density (n_e) dependence of the shinethrough heat load on the wall (P_{wall}) for 16.5MW D^0 beam injection in Scenario 2 (Q=10, P_{fus}=400MW, 400sec burn) is shown for E_B = 0.25, 0.5, 0.75 and 1 MeV in Fig. 1 (a). Thus the 1 MeV NB can start injection at n_e = 5x19/m^3. Figure 1 (b) shows operation space for DT plasmas defined by the shinethrough limit, n_e limit and the L-H transition boundary (P_{inj}/P_{LH}=1). The NB injection start point at n_e = 5x19/m^3 is well above the Type I – Type III ELM boundary (P_{inj}/P_{LH}=1.5) and hence a good H-mode would be expected.

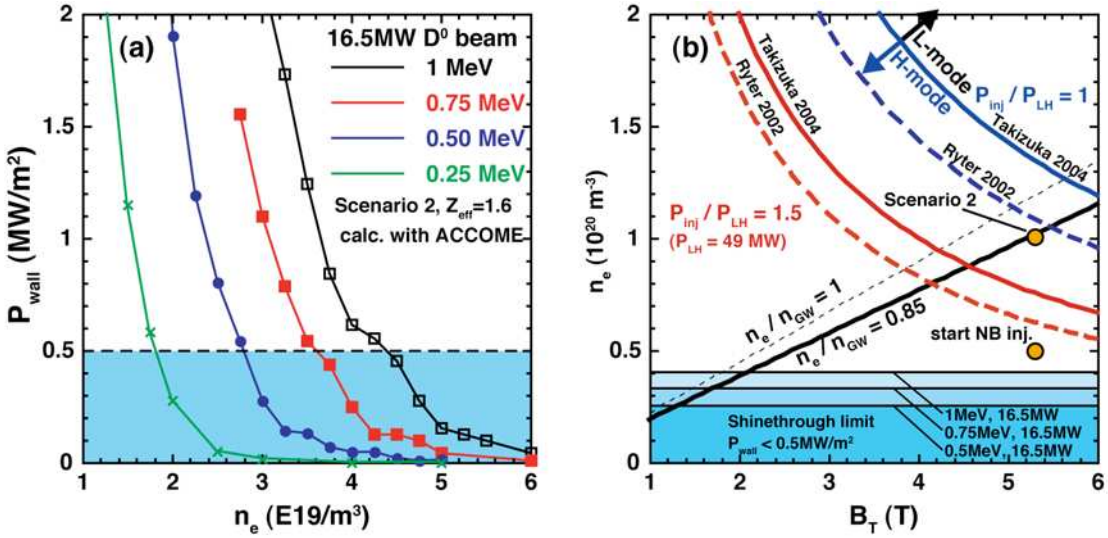

Fig.1 (a) Electron density dependence of the shinethrough heat load on the far wall (P_{wall}) for 16.5 MW D^0 beam injection to Ref. Scenario 2 at 0.25, 0.5, 0.75 and 1 MeV. (b) DT operation space defined by the shinethrough limit, density limit and L-H transition boundary, where the total injection power (P_{inj}) is 73MW and q_{95}=3.

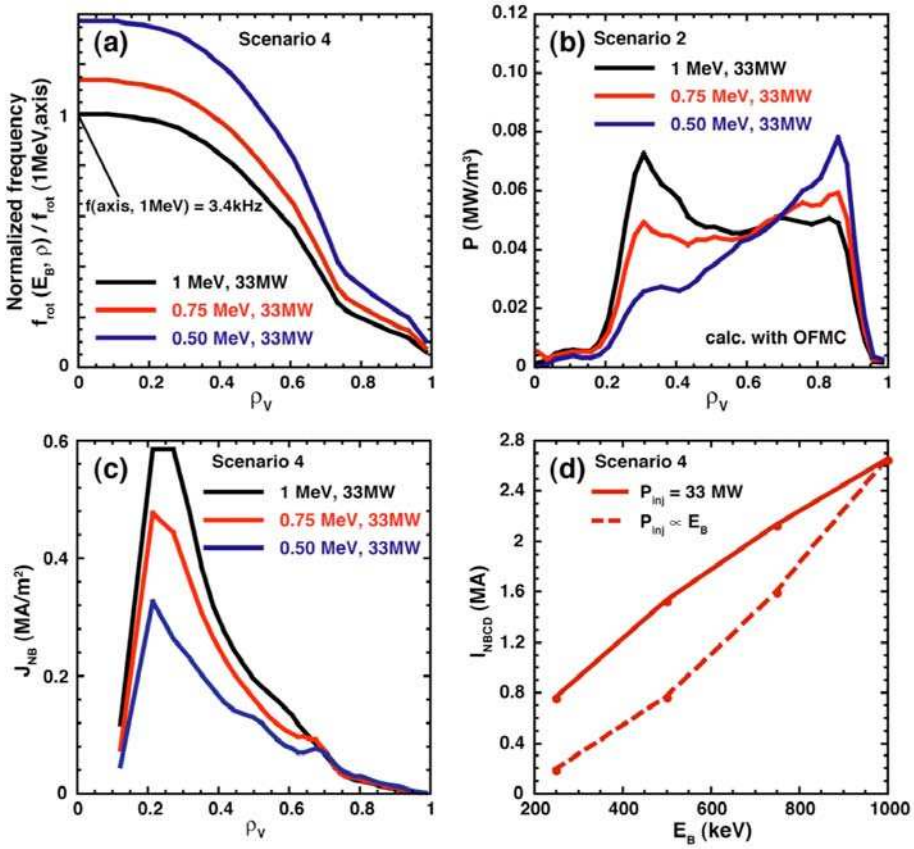

Fig.2 (a) Toroidal rotation frequency profiles for Ref. Scenario 4, (b) heating profiles for Ref. Scenario 2 and (c) NBCD profiles by 2 NBIs (33MW) at 0.5, 0.75 and 1 MeV. (d) Beam energy dependeces of the total NBCD for Ref. Scenario 4 by the 33MW constant P_{inj} (solid) and the beam energy proportional P_{inj} (dashed).

Here the Takizuka [1] and Ryter [2] scalings are employed for the L-H transition power and the total auxiliary heating power is 73 MW delivered by 2 NBIs (33MW), ion cyclotron heating (20MW) and electron cyclotron heating (20MW).

Profiles of the toroidal rotation and NB driven current density (J_{NB}) in Scenario 4 (Q=5, steady-state) and heating profiles in Scenario 2 for E_B = 0.5, 0.75 and 1 MeV are shown in Fig. 2(a), (c) and (b), respectively. Here the constant injection power 33MW (16.5MW/injector x 2NBIs) is assumed. Although the rotation increases by 13% at 750keV relative to 1MeV, NB current drive (NBCD) decreases by 20%, which would be problematic for the development of steady-state scenarios. Figure 2 (d) shows the E_B dependences of NBCD for Scenario 4 with two assumptions on P_{inj}, i.e. the constant power and the beam energy proportional power. Reduction of the NBI central heating at high density necessary for the ITER mission is significant at 500keV, confirming the need for higher energy in DT operation, while the beam energy should be limited to 500keV due to the shinethrough loading on the wall in hydrogen operation.

Neutral beam power variation during a pulse enables the plasma beta control for avoiding the stability boundary. Such a variation can be done by changing the beam energy in

real-time. The 1 MeV injector can change the energy by ~25%. Since P_{inj} is proportional to $E_B^{2.5}$, P_{inj} can be reduced down to half at 750 keV. The plasma stored energy (W_{ST}) control is simulated with a 0D model. For given waveforms of the reference W_{ST} and the energy confinement time (τ_E), time evolution of W_{ST} is simulated with the PD (Proportional and Differential) control scheme. A simulation result is shown in Fig. 3. Here one injector is assigned to the W_{ST} feedback control, and the other injector is for feedforward injection at 1 MeV and 16.5 MW. The stored energy successfully traces the preprogrammed waveform (Fig. 3(a)). The total injection power and the beam energy of the NB injector assigned for control are shown in Fig. 3 (b) and (c), respectively.

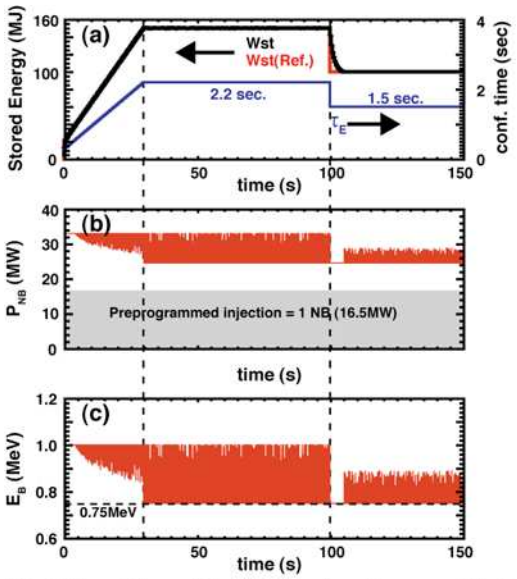

Fig.3 Simulation of the plasma stored energy (W_{ST}) FB control. (a) Reference (black) and calculated (red) W_{ST} and energy confinement time (τ_E). (b) Total NB power. (c) FB controlled beam energy.

2. NBCDC code benchmark

The Fokker-Planck code ACCOME [3] is benchmarked against the orbit following Monte-Carlo code OFMC [4] for Scenario 4. The OFMC code includes the orbit effects in a toroidal system, such as displacement of a particle orbit from a magnetic surface, particle trapping and variation of the pitch angle in a bounce motion along a magnetic field line. The ACCOME code adopts numerically derived eigenfunctions of the bounce-averaged, two-dimensional Fokker-Planck equation [5]. The fast ion source profile is also bounce-averaged. Figure 4(a) shows a comparison of the fast ion current density ($j_{f//}$) profile. Although the profiles agree rather well, the OFMC profile is slightly wider than the ACCOME one. The difference in the total fast ion current is ~ 15 %.

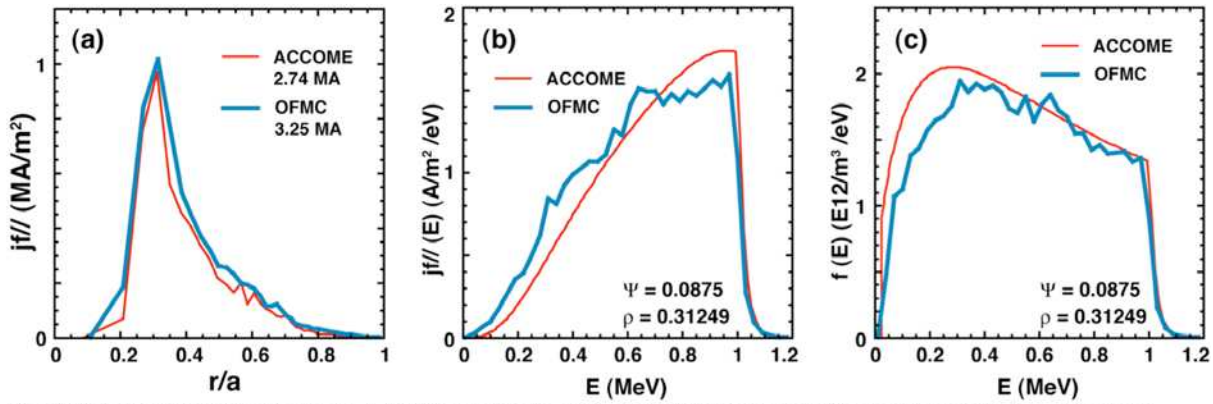

Fig.4 (a) The fast ion current density ($j_{f//}$). (b) The contribution to $j_{f//}$ and (c) the fast ion distribution function in the energy space.

The energy spectrum of the contribution to the fast ion current $j_{f//}(E)$ and distribution function $f(E)$ are compared in Fig. 4(b) and (c), respectively. In E < 0.6 MeV, $j_{f//}(E)$ by OFMC is larger than that by ACCOME even though f (OFMC) is smaller than f(ACCOME). This indicates the diffusion in the pitch angle (ξ) space is different.

The bounce average treatment and the finite banana width effect are examined by the point source method (fast ion produced at a given location and with a given ξ). The ξ dependence of NBCD for the point source at (R, Z)=(7.98, -0.42) corresponding to ρ=0.9 is compared by turning off the finite banana width effect (w_B=0) in OFMC (Fig. 5(a)). The bounce average treatment in ACCOME agrees well with OFMC. The bounce average effect is also compared for point sources along the beam line in Fig. 5(b). Discrepancy between ACCOME and OFMC(w_B=0) becomes large in ρ<0.6. Comparison between OFMC($w_B\neq0$) and OFMC(w_B=0) in Fig. 5(b) shows the finite banana width effect is not negligible. Thus for improving the Fokker-Planck method, inclusion of the finite banana width effect and re-examination of the bounce average treatment are principal subjects. The different diffusion in the ξ space mentioned above could be improved by a refined bounce average treatment.

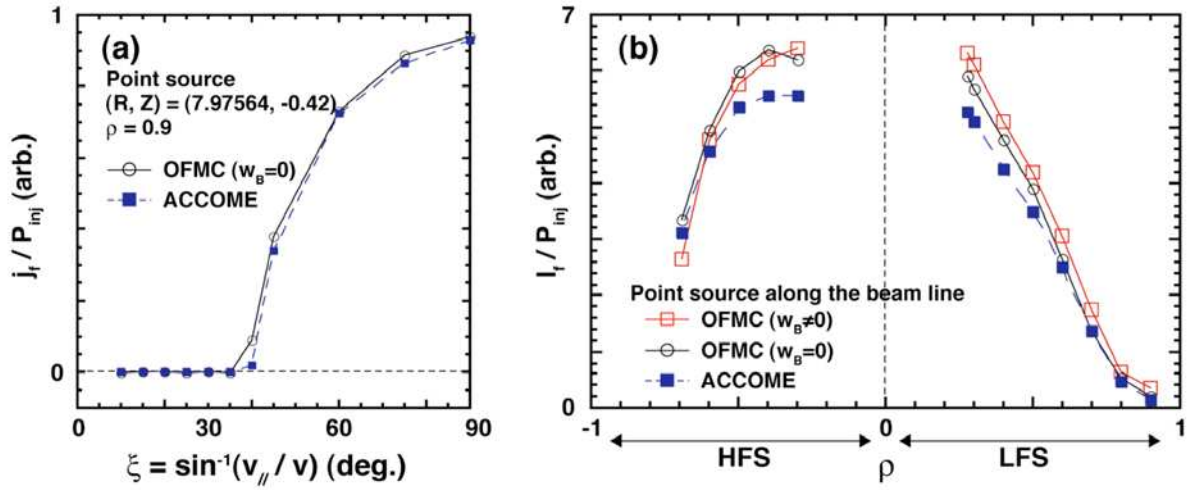

Fig.5 ACCOME - OFMC comparions. (a) Pitch angle (ξ) dependece of the NBCD for the given point source of the fast ions at (R, Z)=(7.96, -0.42), where the finite banana width effect turned off in OFMC. (b) NBCD for point sources along the NB trajectory.

References

[1] T. Takizuka, PPCF 46, A227 (2004).

[2] F. Ryter and H-mode Threshold Database Group, PPCF 44, A415 (2002).

[3] K. Tani, M. Azumi, R. S. Devote, Journal of Computational Physics 98, 332(1992).

[4] K. Tani, et al., Journal of Phys. Soc. Jpn. 50, 1726 (1981).

[5] J.G. Cordey, Nucl. Fusion 16, 499 (1976).